0026-895X/06/6905-1518–1526$20.00
MOLECULAR PHARMACOLOGY
Copyright © 2006 The American Society for Pharmacology and Experimental Therapeutics
Mol Pharmacol 69:1518–1526, 2006

Vol. 69, No. 5
19844/3098708
Printed in U.S.A.

Molecular Determinants in the Second Intracellular Loop of the 5-Hydroxytryptamine-1A Receptor for G-Protein Coupling[S]

Neena Kushwaha, Shannon C. Harwood, Ariel M. Wilson, Miles Berger, Laurence H. Tecott, Bryan L. Roth, and Paul R. Albert

Ottawa Health Research Institute (Neuroscience) and Department of Cellular and Molecular Medicine, University of Ottawa, Ottawa, Ontario, Canada (N.K., S.C.H., A.M.W., P.R.A.); Department of Psychiatry, Center for Neurobiology and Psychiatry, Institute for Neurodegenerative Diseases, University of California, San Francisco School of Medicine, San Francisco, California (M.B., L.H.T.); and Department of Biochemistry, Case Western Reserve University Medical School, Cleveland, Ohio (B.R.L.)

Received October 12, 2005; accepted January 12, 2006

ABSTRACT

This study provides the first comprehensive evidence that the second intracellular loop C-terminal domain (Ci2) is critical for receptor-G protein coupling to multiple responses. Although Ci2 is weakly conserved, its role in 5-hydroxytryptamine-1A (5-HT1A) receptor function was suggested by the selective loss of G$\beta\gamma$-mediated signaling in the T149A-5-HT1A receptor mutant. More than 60 point mutant 5-HT1A receptors in the α-helical Ci2 sequence (^{143}DYVNKRTPRR^{152}) were generated. Most mutants retained agonist binding and were tested for G$\beta\gamma$ signaling to adenylyl cyclase II or phospholipase C and Gαi coupling to detect constitutive and agonist-induced G_i/G_o coupling. Remarkably, most point mutations markedly attenuated 5-HT1A signaling, indicating that the entire Ci2 domain is critical for receptor G-protein coupling. Six signaling phenotypes were observed: wild-type-like, Gα_i-coupled/weak G$\beta\gamma$-coupled, G$\beta\gamma$-uncoupled, G$\beta\gamma$-selective coupled, uncoupled, and inverse coupling. Our data elucidate specific roles of Ci2 residues consistent with predictions based on rhodopsin crystal structure. The absolute coupling requirement for lysine, arginine, and proline residues is consistent with a predicted amphipathic α-helical Ci2 domain that is kinked at Pro150. Polar residues (Thr149, Asn146) located in the externally oriented positively charged face were required for G$\beta\gamma$ but not Gα_i coupling, suggesting a direct interface with G$\beta\gamma$ subunits. The hydrophobic face includes the critical Tyr144 that directs the specificity of coupling to both G$\beta\gamma$ and Gα_i pathways. The key coupling residues Tyr144/Lys147 (Ci2) are predicted to orient internally, forming hydrogen and ionic bonds with Asp133/Arg134 (Ni2 DRY motif) and Glu340 (Ci3) to stabilize the G-protein coupling domain. Thus, the 5-HT1A receptor Ci2 domain determines G$\beta\gamma$ specificity and stabilizes Gα_i-mediated signaling.

The receptor domains that mediate coupling to Gα-induced responses have been intensively studied, but determinants of G$\beta\gamma$ signaling have yet to be addressed (Bourne, 1997; Meng and Bourne, 2001; Sakmar et al., 2002). Deletion and point mutagenesis studies have indicated that the N- and C-terminal portions of the i3 domain (Ni3, Ci3) and the i2 and C-terminal regions play important roles in receptor coupling to G-proteins. Using a saturation mutagenesis approach to study the G_q-coupled m5-muscarinic receptor, the i2 and Ni3 domains were predicted to form an amphipathic α-helical structure, with charged residues of Ni3 recruiting G-proteins to form interactions with embedded hydrophobic residues (Burstein et al., 1996, 1998; Hill-Eubanks et al., 1996). Likewise, saturation and cysteine mutagenesis of the Ci3 domain (near TMIV) suggests an α-helical structure containing residues that interact with G-protein and intracellular receptor domains to regulate constitutive activity (Liu et al., 1995; Spalding et al., 1998; Zeng et al., 1999; Shi et al., 2002; Schmidt et al., 2003). The crystal structure of *cis*-retinal-bovine rhodopsin (inactive state) (Palczewski et al., 2000) has revealed some intramolecular interactions that are believed to lock the receptor in an inactive state, especially between

This work was supported by a grant from the Canadian Institutes of Health Research (CIHR) (to P.R.A.) and a CIHR Doctoral Award (to N.K.). P.R.A. is the CIHR/Novartis Michael Smith Chair in Neuroscience. M.B. was supported by a National Institute of Mental Health National Research Service Award (F31-MH075708-01) and the Medical Scientist Training Program at the University of California, San Francisco. L.H.T. was supported by the National Institutes of Health (NIH), and B.L.R. was supported by NIH grants MH57635 and K02-MH01366.

[S] The online version of this article (available at http://molpharm.aspetjournals.org) contains supplemental material.

Article, publication date, and citation information can be found at http://molpharm.aspetjournals.org.
doi:10.1124/mol.105.019844.

ABBREVIATIONS: Ci2, C-terminal of the i2 loop; Ci3, C-terminal of the i3 loop; 8-OH-DPAT, 8-hydroxy-2-(di-*n*-propylamino)tetralin; Ni2, N-terminal of the i2 loop; Ni3, N-terminal of the i3 loop; AC, adenylyl cyclase; DPAT, dipropylaminotetralin; HEK, human embryonic kidney; DMEM, Dulbecco's modified Eagle's medium; wt, wild type; GPCR, G-protein-coupled receptor; 5-HT, 5-hydroxytryptamine.

the conserved (D/E)RY motif at TM3/Ni2 and a conserved aspartic acid/glutamic acid residue of Ci3/transmembrane 6 (Zeng et al., 1999; Ballesteros et al., 2001; Meng and Bourne, 2001). Although the importance of the conserved (D/E)RY motif in the Ni2 region in receptor activation has been examined extensively (Meng and Bourne, 2001; Sakmar et al., 2002), the structure and importance of the adjacent Ci2 domain in coupling has yet to be addressed. Random mutagenesis of the m5-muscarinic i2 domain yielded few functional mutants of the Ci2 region (Burstein et al., 1998), suggesting the potential importance of this domain in coupling. However, their $G\alpha_q$-mediated signaling screen did not select nonfunctional mutants; hence, no firm conclusion could be reached regarding Ci2 function. Furthermore, previous receptor mutagenesis studies have not addressed $G\beta\gamma$-mediated signaling, which increasing evidence suggests can be dissociated from $G\alpha$-mediated coupling (Chidiac, 1998; Albert and Robillard, 2002).

Hence, we examined in detail the role of the Ci2 domain in 5-HT1A receptor coupling to both $G\alpha_i$ and $G\beta\gamma$-mediated signaling pathways. The 5-HT1A receptor is a G_i/G_o-coupled receptor that is a critical regulator of the brain serotonergic system and has been implicated in mental illnesses such as depression and anxiety (Pineyro and Blier, 1999; Albert and Lemonde, 2004; Gross and Hen, 2004). In previous studies, we found that the mutation of a single threonine residue (T149A) within the Ci2 region reduced or blocked 5-HT1A receptors from coupling to several $G\beta\gamma$-mediated pathways but not to $G\alpha_i$-mediated inhibition of forskolin or G_s-stimulated adenylyl cyclase activation (Lembo et al., 1997; Albert et al., 1998; Liu et al., 1999). The affected $G\beta\gamma$ pathways included phospholipase C-mediated calcium mobilization (Lembo et al., 1997; Wurch et al., 2003; Kushwaha and Albert, 2005), inhibition of dihydropyridine-induced (L-type) and N-type calcium channel activation (Lembo et al., 1997; Wu et al., 2002), and constitutive activation of adenylyl cyclase II (Albert et al., 1999). The T149A mutation also blocked 5-HT1A-mediated mitogen-activated protein kinase inhibition in raphe RN46A cells (Kushwaha and Albert, 2005). Thus, the T149A residue of the Ci2 domain plays a crucial role in $G\beta\gamma$-induced pathways of the 5-HT1A receptor. In addition to the i2 domain, the i3 and palmitoylated C-terminal domains of the 5-HT1A receptor have also been implicated in G-protein coupling (Varrault et al., 1994; Sun and Dale, 1999; Papoucheva et al., 2004; Turner et al., 2004). Peptides derived from the Ni3 or Ci3 domains of the 5-HT1A receptor can mimic $G\alpha_i$-mediated inhibition of adenylyl cyclase, whereas i2 peptides prevented this coupling (Varrault et al., 1994; Ortiz et al., 2000). This suggests that Ni3 and Ci3 domains may mediate the activation of $G\alpha_i$, whereas the i2 loop is involved in receptor interaction with $G\alpha_i$ but not in its activation.

Computer-based analysis predicts that the Ci2 domain has an amphipathic α-helical structure that is conserved among many G-protein-coupled receptors (GPCRs) (Albert et al., 1998). To provide insight into the structural determinants of the Ci2 loop and empirical validation of their importance for 5-HT1A receptor coupling to G-protein signaling, we have generated a series of random targeted point mutants of nine critical i2 residues that are predicted to form the amphipathic α-helical domain. Based on the coupling of tolerated substitutions, we have used computer modeling to identify critical amino acid side chain interactions that are implicated in $G\alpha_i$ and $G\beta\gamma$ signaling of the receptor. Using this approach, we have provided the first comprehensive insights into the role of the Ci2 domain in both $G\alpha$ and $G\beta\gamma$ signaling.

Materials and Methods

Materials. All chemicals were reagent grade. Forskolin, 3-iso-butyl-1-methylxanthine, 4-methylumbelliferyl-β-D-galactosidase, 5-HT, pertussis toxin, EGTA, and 8-OH-DPAT were purchased from Sigma (St. Louis, MO). Fura-2-acetoxymethyl ester was obtained from Invitrogen (Mississauga, ON, Canada). ^{125}I-Succinyl cAMP (2200 Ci/mmol) was purchased from PerkinElmer Life and Analytical Sciences (Boston, MA). Anti-3′, 5′-cAMP antibody was obtained from MP Biomedicals, Inc. (Aurora, OH). The QuikChange XL site-directed mutagenesis kit was obtained from Stratagene (La Jolla, CA).

Plasmids. To generate the 5-HT1A expression plasmids, a 1.9-kilobase BamHI/XbaI fragment of the rat 5-HT1A receptor gene wild-type (1A) or receptor mutant (T149A-i2) were subcloned into BamHI/XbaI-digested pcDNA3 (Invitrogen). For construction of 5-HT1A-i2 mutant receptors, single point mutations of each amino acid in the 5-HT1A-i2 loop sequence DYVNKRTPRR were generated randomly using a primer-directed mutagenesis kit (QuikChange XL site-directed mutagenesis kit; Stratagene). For example, to generate 5-HT1A receptors mutated at Thr149, the following oligonucleotides were used: sense, 5′-TATAGACTATGTGAACAAAAGG**NNG**CCCCGG-3′; and antisense, 5′-CGCGCCGGGG**CNN**CCTTTTGTTCACATAGTC-3′. Mutant primers used for each i2 loop residue are listed in Supplemental Table S1. Using the wild-type 5-HT1A cDNA (described above) as a template, we prepared the sample reactions according to the manufacturer's protocol and used the recommended cycling parameters to amplify polymerase chain reaction products. The receptor mutants were identified using Sanger dideoxynucleotide termination DNA sequencing method with the following primer located 40 to 80 nucleotides adjacent to the sites of the mutation: 5′-CTGTGCTGCACCTCGTCCATCCTG-3′.

Cell Culture and Transfection. Human embryonic kidney (HEK) 293 cells were maintained in DMEM (Wisent, St. Bruno, QC, Canada) plus 7% fetal bovine serum (Invitrogen) at 37°C in 5% CO_2. HEK 293 cells were plated at 7×10^6 cells/10-cm dish and incubated overnight. For measurement of constitutive 5-HT1A receptor activity, cells were transiently transfected by calcium phosphate coprecipitation with 12 μg each of the indicated plasmids (adenylyl cyclase II, $G\alpha i2$, and 5-HT1A-wt or 5-HT1A-i2 mutant receptor), and 6 μg of pCMV-βGAL in 7 ml/dish DMEM + 10% fetal calf serum, and 20 mM HEPES, pH 7.0, at 37°C (5% CO_2) for 4 to 6 h. Consistent basal cAMP levels were observed between wt and mutant receptors, indicating similar levels of adenylyl cyclase II expression between transfections. To measure the inhibition of dopamine-stimulated cAMP formation by 5-HT1A receptor activation, HEK 293 cells were transiently transfected with 12 μg of both the human dopamine-D1 and rat 5-HT1A receptors. The cells were then plated onto six-well plates for cAMP and β-galactosidase assays. Consistent dopamine responses were obtained among wt and mutant receptors, indicating equivalent expression levels of the D1 receptor coupling between transfections. Ltk− cells were cultured in α-minimal essential medium (Wisent) supplemented with 5% fetal bovine serum at 37°C (5% CO_2). For intracellular calcium measurements Ltk− cells were transiently transfected with 5 μg of either 5-HT1A-wt or 5-HT1A-i2 mutant receptors using Lipofectamine Plus reagents (Invitrogen) according to the manufacturer's protocol. Cells were harvested after 48 h for intracellular calcium measurements. In parallel experiments, membranes were prepared from Ltk− cells transiently transfected with the indicated 5-HT1A mutant receptors and subjected to binding analysis with [^{3}H]8-OH-DPAT.

cAMP Assay. Measurement of cAMP was performed as described previously (Albert et al., 1998). In brief, 24 h after plating HEK cells

into six-well dishes, the cells were washed once with serum-free DMEM and incubated in 1 ml/well DMEM, 20 mM HEPES, pH 7.0, and 100 μM 3-isobutyl-1-methylxanthine for 15 to 20 min at 37°C. Experimental compounds were added to triplicate wells, as indicated. Media were collected, centrifuged at 14,000*g* (30 s) to remove floating cells, and the supernatant was stored at −20°C until assayed for cAMP using a specific radioimmunoassay (MP Biomedicals) as described previously (Albert et al., 1998). Attached cells were harvested using reporter lysis buffer (Promega), centrifuged for 2 min at 4°C, and stored at −20°C. Transfection efficiency was monitored by cotransfection of β-galactosidase plasmid and cAMP values were normalized to β-gal activity (Albert et al., 1999). Pertussis toxin (50 ng/ml) was present overnight (16 h) in indicated samples.

β-Galactosidase Assay. Transfection efficiencies were monitored by β-galactosidase assay. The transfected cells were rinsed with phosphate-buffered saline, resuspended in 200 μl of reporter lysis buffer, incubated for 15 min at room temperature, scraped, frozen, and thawed to complete cell lysis. The lysates were centrifuged (14,000 rpm, 2 min, 4°C) and the supernatant was recovered for the measurement of β-galactosidase activity. Equal volumes (30 μl each) of cell extract and 0.3 mM 4-methylumbelliferyl-β-D-galactosidase substrate in 15 mM Tris, pH 8.8, were mixed gently, incubated in the dark at 37°C for 30 min, and the reaction was terminated upon the addition of 50 μl of stop solution (300 nM glycine and 15 mM EDTA, pH 11.2). The sample was transferred to 2 ml of Z buffer (60 mM Na_2HPO_4, 40 mM NaH_2PO_4, 10 mM KCl, and 1 mM $MgSO_4$), and the fluorescence was measured at λ_{EX} = 350 nm, λ_{EM} = 450 nm on a PerkinElmer LS-50 spectrofluorometer (Beaconsfield, Buckinghamshire, UK). The average β-galactosidase activity for transfection of mutant receptor plasmids in each experiment ranged from 0.8- to 1.3-fold of that for wild-type receptor.

Ligand Binding. Cell membranes were prepared from transfected cultures on 15-cm dishes by replacing the growth medium with ice-cold hypotonic buffer (15 mM Tris-HCl, pH 7.4, 2.5 mM $MgCl_2$, and 0.2 mM EDTA). After swelling for 10 to 15 min at 4°C, the cells were scraped from the plates, sonicated on ice, centrifuged (14,000 rpm for 20 min), and resuspended in ice-cold buffer (75 mM Tris-HCl, pH 7.4, 12.5 mM $MgCl_2$, and 1 mM EDTA). Aliquots of thawed and sonicated membrane preparation (100 μg/tube) were added to triplicate tubes containing 200 μl of buffer (75 mM Tris-HCl, pH 7.4, 12.5 mM $MgCl_2$, and 1 mM EDTA) and 10 nM [^{3}H]8-OH-DPAT (GE Healthcare, Little Chalfont, Buckinghamshire, UK) without or with 5-HT (10 μM) to determine total versus nonspecific binding at room temperature (30 min). Reactions were terminated by filtration through GF/C (Whatman, Clifton, NJ) filters, washing with 3 × 4 ml of ice-cold buffer (50 mM Tris-HCl, pH 7.4), and 3 ml of scintillation fluid added to filters to quantify radioactivity by liquid scintillation counting. Protein was assayed with the BCA protein assay kit (Pierce, Rockford, IL) with bovine serum albumin as a standard.

Measurement of Intracellular Calcium. As described previously (Liu and Albert, 1991), cells were grown to 80% confluence, harvested with trypsin/EDTA, resuspended in 3 ml of serum-free DMEM with the calcium indicator Fura-2-acetoxymethyl ester (3 μM), and incubated for 30 min at 37°C with shaking (100 rpm). The cells were washed once with 20 mM HEPES, pH 7.2, 0.1 M NaCl, 4.6 mM KCl, 10 mM D-glucose, and 1 mM $CaCl_2$, pH 7.4, resuspended in 2 ml of buffer, and subjected to fluorometric measurement. Changes in the fluorescence ratio was recorded on a PerkinElmer Cetus LS-50 spectrofluorometer and analyzed by computer based on a K_d value of 227 nM for the Fura-2/Ca^{2+} complex. Calibration of R_{max} was performed by the addition of 0.1% Triton X-100 and 20 mM Tris base and of R_{min} by the addition of 10 mM EGTA. Experimental compounds were added directly to cuvette at the specified concentrations at the indicated times.

Statistical Analysis. The data are presented as mean ± S.E.M. of at least three independent experiments. Statistical analyses of the data were done using Prism software (GraphPad Software Inc., San Diego, CA).

Modeling. A preliminary model of the rat 5-HT1A receptor (inactive state) was prepared using bovine rhodopsin as a template using methods similar to those described previously (Shapiro et al., 2002; Setola et al., 2005). The full details of the model will be described in a subsequent publication.

Results

Mutagenesis Strategy. We used a random primer-based mutagenesis approach to incorporate point mutations tar-

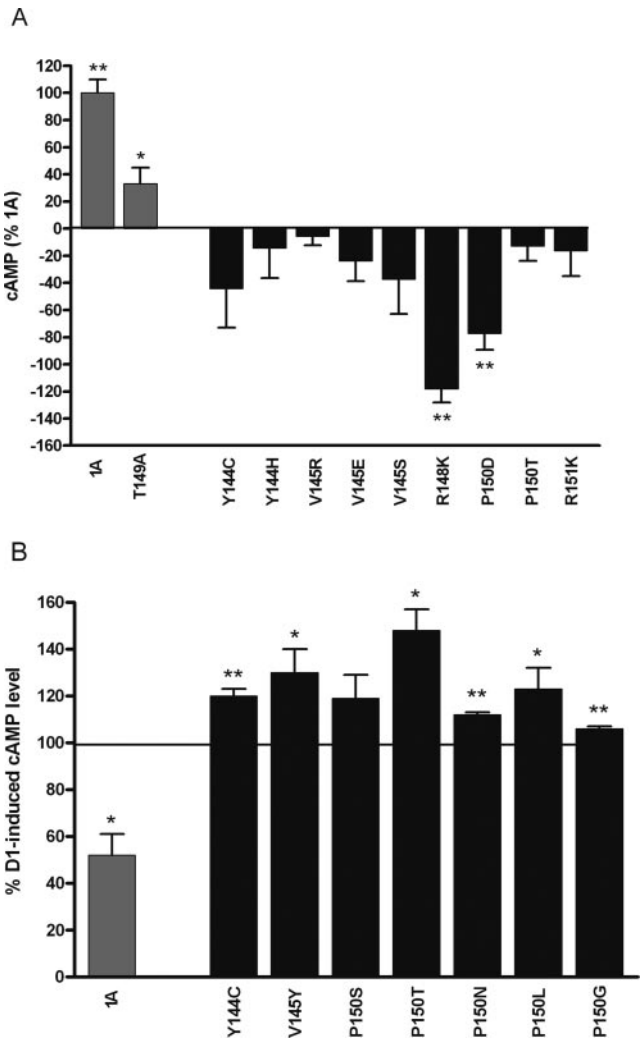

Fig. 1. Inverse agonist function of 5-HT1A-i2 mutant receptors on Gαi and G$\beta\gamma$ responses. A, agonist-independent G$\beta\gamma$-mediated activation of adenylyl cyclase II. HEK 293 cells were transiently transfected with expression plasmids for adenylyl cyclase II, $G\alpha_{i2}$, and the indicated wild-type (1A) or i2 mutant 5-HT1A receptors, and agonist-independent cAMP production was measured. Constitutive receptor activity was determined using the average difference between pertussis toxin-treated and non-treated cells normalized to wild-type 5-HT1A activity (100%) for three to six independent experiments. A significant difference of receptor activity from 0 (pertussis toxin-treated) was calculated using paired *t* test: **, $p < 0.01$; *, $p < 0.05$. B, agonist-induced inhibition of G_s-stimulated cAMP accumulation. HEK 293 cells were transiently cotransfected with expression plasmids for dopamine-D1 receptor and wild-type or mutant 5-HT1A receptor. Cells were treated with dopamine agonist apomorphine (10 μM) (control) or apomorphine and 5-HT1A agonist 8-OH-DPAT (1 μM), and cAMP was measured. Values were normalized to apomorphine-stimulated cAMP accumulation (100%). Significant differences from 100% were calculated using paired *t* test: **, $p < 0.01$; *, $p < 0.05$.

geted at the 5-HT1A-i2 loop sequence ^{143}DYVNKRTPRR^{152}, a region implicated in G-protein coupling of the receptor (Albert et al., 1998). The function of mutant receptors was examined using three rapid functional assays in transiently transfected cells: coupling to adenylyl cyclase II, or coupling to phospholipase Cβ (both G$\beta\gamma$-mediated), or inhibition of G_s-stimulated adenylyl cyclase activation (Gα_i-mediated). Each of these 5-HT1A receptor-mediated signals is blocked by pertussis toxin treatment, indicating an obligatory role for G_i/G_o proteins. Constitutive coupling to adenylyl cyclase II was assessed in HEK 293 cells cotransfected with 5-HT1A receptor, adenylyl cyclase II, and Gα_{i2}, which results in an agonist-independent increase in cAMP that is mediated by G$\beta\gamma$ signaling and is reduced in the T149A 5-HT1A receptor mutant (Albert et al., 1999) (Fig. 1A). In this model, the addition of agonist does not increase cAMP any further, hence constitutive receptor coupling is measured. Agonist-mediated 5-HT1A receptor signaling to phospholipase Cβ was assayed by measuring DPAT-induced calcium mobilization in transfected Ltk− fibroblast cells, a G$\beta\gamma$-mediated pathway that is reduced by the T149A mutation (Lembo et al., 1997) (Fig. 2). Coupling of 5-HT1A receptors to Gα_i (Liu et al., 1999) was examined by assaying agonist-mediated inhibition of G_s-stimulated (via D1 receptor) cAMP accumulation in transfected HEK 293 cells (Albert et al., 1999) (Fig. 1B).

Mutant Phenotypes. Overall, 61 mutant receptors were generated and examined using the screening assays described above, and these data are assembled in Table 1. Most of the mutants displayed significant levels of specific binding ([^{3}H]8-OH-DPAT) that was comparable with that of nonmutated 5-HT1A receptors (Table 1). Some mutants displayed variation in binding levels because of transfection efficiency, but all displayed at least one functional response except for one case (K147Q), indicating that these mutant receptors folded correctly and were functional. In addition, the level of basal and dopamine-stimulated cAMP was similar in transfections of different mutants (data not shown), indicating consistent levels of adenylyl cyclase II or D1 receptor coupling among transfections. The majority (44 of 61) of the mutant receptors remained significantly coupled to Gα_i-mediated inhibition of cAMP accumulation (Table 1). G$\beta\gamma$-signaling of mutant receptors, such as phospholipase Cβ-mediated calcium mobilization, was blocked by pertussis toxin (Fig. 2), indicating mediation by G_i/G_o proteins. The mutant 5-HT1A receptors were classified into six main signaling phenotypes (Table 2): wild-type-like (3 of 61; T149R,G and N146T); Gα_i-coupled/weak G$\beta\gamma$-coupled (8 of 61; T149AEQ, V145LK, R148G, and R151AT); G$\beta\gamma$-uncoupled (16 of 61); G$\beta\gamma$-selective coupled (16 of 61); uncoupled (17 of 61); and a few mutants displayed inverse basal activity to inhibit adenylyl cyclase II (Fig. 1A) or mediated inverse agonist activity to potentiate D1-induced adenylyl cyclase activation (Fig. 1B). Only two mutants were identified (R152N/D) that lacked Gα_i coupling and retained minimal G$\beta\gamma$ coupling, indicating an important role for the Ci2 domain in G$\beta\gamma$ coupling. Within the G$\beta\gamma$-coupled group of receptors, signaling to adenylyl cyclase II or phospholipase C was selectively preserved depending on the mutation, and in several cases, Gαi signaling was also preserved (Table 2). At other sites in the i2 domain, most mutants were nonfunctional, suggesting that very few mutations preserve the i2 structure required for proper G-protein coupling.

Predicted Structures. Because 5-HT1A-i2 peptides mimic 5-HT1A receptor coupling to inhibition of adenylyl cyclase (Varrault et al., 1994; Thiagaraj et al., 2002) and trigger G$\beta\gamma$-mediated calcium mobilization (N. Kushwaha and P. R. Albert, unpublished data), we examined the predicted peptide secondary structures of the mutant Ci2 domains. The presence of a predicted amphipathic α-helical structure (Albert et al., 1998) was not altered by any of the point mutations of the Ci2 domain. Garnier-Robson analysis (Supplemental Table S2) revealed a predicted coil at Thr149/Pro150. Any mutant predicted to be disrupted, displaced, or even reduced at the Thr149/Pro150 coil domain (T149AQWVM, all Pro150 mutants, V145KYES, N146A, R148LQV, R151AMLK, R152VA) displayed impaired coupling to G$\beta\gamma$ or to both Gα_i and G$\beta\gamma$ signaling (Table 1). Strikingly, any substitution at residue Pro150 (Table 1) was completely disrupted of receptor function and was predicted to disrupt the predicted coil structure in the i2 peptide (Sup-

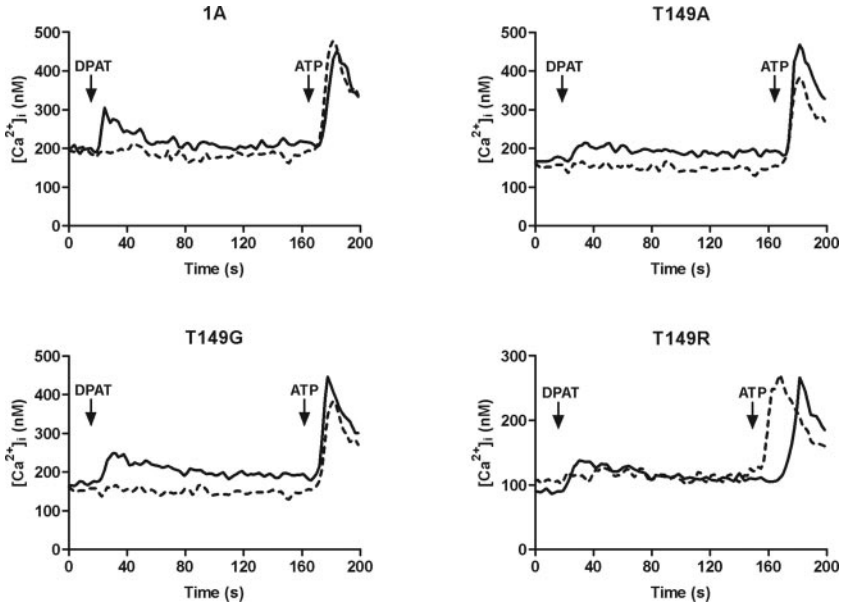

Fig. 2. Coupling of 5-HT1A-i2 mutants to calcium mobilization is G_i/G_o-specific. Fibroblast Ltk− cells were transiently transfected with either 5 μg of wild-type 5-HT1A (1A) or 5-HT1A-i2 T149 mutant receptors [i2 (T149A), glycine (T149G), arginine (T149R)], and changes in intracellular free calcium concentration in response to 5-HT1A agonist DPAT (1 μM; solid line) were measured (see *Materials and Methods*). Calcium mobilization of the wild-type (1A) and mutant 5-HT1A receptors was blocked by pretreatment with pertussis toxin (50 ng/ml, 16 h; broken line). Response to ATP (10 μM; solid line) was used as a positive control. Traces shown are representative; similar results were obtained from at least three independent experiments.

TABLE 1

Summary of binding, $G\alpha_i$-, and $G\beta\gamma$-coupling properties of 5-HT1A-i2 mutants

Agonist-induced changes in intracellular free calcium concentration in Ltk− cells transiently transfected with wild-type 5-HT1A (1A) or 5-HT1A-i2 mutant receptors were measured and quantified as the percentage of control over basal $[Ca^{2+}]_i$ levels (column 1). In parallel experiments, membranes were prepared from Ltk− cells transiently transfected with the indicated 5-HT1A mutant receptors and were subjected to binding analysis with [^{3}H]8-OH-DPAT (column 2). Agonist-independent $G\beta\gamma$-mediated activation of adenylyl cyclase II was determined using HEK 293 cells transiently transfected with expression plasmids for adenylyl cyclase II, $G\alpha_{i2}$, and the indicated wild-type (1A) or i2 mutant 5-HT1A receptor. Agonist-independent cAMP production was determined using the average difference between pertussis toxin-treated and nontreated cells for three to six independent experiments, where (+++) indicates ≥80%, (++) ≥50%, and (+) between 19 and 27% increase in cAMP production compared with wild-type 5-HT1A receptor, and − indicates no detectable activity (column 3). For $G\alpha_i$-mediated inhibition of adenylyl cyclase, HEK cells were transiently cotransfected with 12 μg of D1 receptor cDNA and an equal amount of wild-type (1A) or 5-HT1A-i2 mutant receptors. Inhibition of D1/$G\alpha_s$-stimulated (10 μM apomorphine) cAMP accumulation by 5-HT1A agonist 8-OH-DPAT (1 μM) was measured by specific radioimmunoassay, and data were presented as the percentage of inhibition of D1-stimulated cAMP levels (column 4). In all cases, data are expressed as mean ± S.E.M. of at least three independent experiments, and values that are significantly different from 0 were identified using Student's paired *t* test and are indicated as ***, $p < 0.001$; **, $p < 0.01$; *, $p < 0.05$.

Substitution	DPAT-Induced $[Ca^{2+}]_i$ (percentage over basal $[Ca^{2+}]_i$)	Receptor Number	Constitutive Activity (Level of Coupling to $\beta\gamma$-Mediated Stimulation of ACII)	Inhibition of D1-Stimulated cAMP Accumulation
	%	*pmol/transfection*		%
WT (1A)	101 ± 8**	1.9 ± 0.4*	+++	48 ± 9*
T149A (i2)	27 ± 9*	2.3 ± 0.7*	+	53 ± 10*
D143F	15 ± 3*	1.5 ± 0.9	−	54 ± 8**
D143V	22 ± 4*	2.5 ± 0.2**	−	56 ± 9**
D143N	26 ± 7*	0.9 ± 0.1 **	−	45 ± 9*
D143L	29 ± 7*	0.7 ± 0.4	−	52 ± 3**
D143C	N.R.	2.9 ± 0.8*	−	44 ± 12*
Y144H	N.R.	1.9 ± 0.2**	−	22 ± 3**
Y144A	4 ± 2	1.7 ± 0.5*	+++	11 ± 8
Y144N	25 ± 7*	2.4 ± 0.6*	−	44 ± 5**
Y144F	N.R.	2.3 ± 0.6*	++	43 ± 7**
Y144V	10 ± 6	2.3 ± 0.2**	−	7 ± 2*
Y144I	N.R.	1.4 ± 0.7	−	26 ± 5*
Y144C	N.R.	2.1 ± 1.1	−	−20 ± 3**
V145L	26 ± 3**	2.2 ± 0.9	+	34 ± 11*
V145K	23 ± 9*	1.4 ± 0.2**	+	41 ± 13*
V145Y	4 ± 3	1.3 ± 0.7	−	−30 ± 10*
V145R	N.R.	1.6 ± 0.6*	−	15 ± 9
V145Q	N.R.	1.9 ± 0.2**	−	27 ± 7*
V145E	12 ± 5	1.8 ± 0.5*	−	32 ± 9*
V145S	N.R.	1.5 ± 0.6*	−	−12 ± 7
V145W	N.R.	1.2 ± 0.2**	−	17 ± 6*
N146T	56 ± 17*	1.8 ± 0.3**	++	31 ± 8*
N146F	14 ± 5*	1.9 ± 0.7*	−	42 ± 10*
N146A	20 ± 13	1.0 ± 0.2*	−	53 ± 10*
K147R	N.R.	2.3 ± 0.6*	−	−3 ± 6
K147Q	N.R.	2.5 ± 1.2	−	−11 ± 9
R148L	17 ± 5*	2.5 ± 0.4**	−	13 ± 4*
R148Q	16 ± 2**	1.3 ± 0.2**	−	20 ± 8*
R148K	12 ± 6	2.1 ± 0.1***	−	4 ± 10
R148E	28 ± 4**	1.5 ± 0.1**	−	20 ± 3**
R148P	N.R.	3.2 ± 0.9*	+	21 ± 4**
R148G	19 ± 6*	2.8 ± 1.1*	+	53 ± 10*
R148V	20 ± 9	1.2 ± 0.4*	−	45 ± 8*
T149E	20 ± 4*	1.0 ± 0.4*	+	50 ± 3**
T149V	10 ± 5	1.7 ± 1.0	−	46 ± 14*
T149G	80 ± 8**	3.3 ± 0.6*	++	52 ± 8**
T149R	50 ± 3**	1.5 ± 0.9	+++	60 ± 8**
T149Q	22 ± 2**	1.8 ± 0.8	+	39 ± 4**
T149M	15 ± 7	1.9 ± 0.2**	−	42 ± 4**
T149W	9 ± 7	2.0 ± 0.7*	−	44 ± 5**
T149P	6 ± 9	2.6 ± 0.4**	++	27 ± 9*
P150R	2 ± 5	2.3 ± 0.1***	−	−6 ± 3
P150N	N.R.	1.3 ± 0.8	−	−12 ± 1**
P150D	N.R.	1.3 ± 0.2**	−	4 ± 2
P150G	N.R.	2.0 ± 1.0	−	−6 ± 1**
P150I	7 ± 8	1.7 ± 0.2**	−	4 ± 1*
P150L	N.R.	0.9 ± 0.6	−	−23 ± 9*
P150F	N.R.	1.9 ± 0.5*	−	15 ± 11
P150S	N.R.	0.8 ± 0.1**	−	−19 ± 10
P150T	N.R.	2.1 ± 0.8*	−	−48 ± 9*
R151Q	4 ± 6	1.7 ± 0.8	−	22 ± 8*
R151A	26 ± 4**	2.3 ± 0.9*	+	24 ± 8*
R151M	8 ± 1**	2.1 ± 1.0	−	20 ± 4*
R151T	27 ± 3**	1.0 ± 0.1**	+	38 ± 7*
R151L	2 ± 5	0.8 ± 0.2*	−	30 ± 6*
R151K	2 ± 4	1.5 ± 1.1	−	26 ± 6*
R152N	16 ± 4*	1.4 ± 0.6	−	10 ± 7
R152V	8 ± 7	1.3 ± 0.5*	−	37 ± 8*
R152A	13 ± 7	2.2 ± 0.9*	−	56 ± 7**
R152P	26 ± 3**	1.1 ± 0.5	−	12 ± 11
R152D	27 ± 6*	1.5 ± 0.8	−	−11 ± 2

N.R., no response to treatments.

plemental Table S2). Conversely, the addition of a proline residue (e.g., R148P, T149P, and R152P) resulted in weakly coupled receptors and an expanded coil domain. In contrast, the predicted hydrophobic α-helix at the start of TMIV (from Arg151 to Ala155) was dispensable for coupling in the T149G/R mutants, whereas several mutants that lacked receptor signaling seemed to retain the TMIV α-helix. Thus, the predicted coil structure at Thr149/Pro150 of the Ci2 domain seems to play a critical role in 5-HT1A receptor signaling.

Inverse Activity. Several mutants displayed inverse activity (Fig. 1). The greatest inverse basal activity toward adenylyl cyclase II was observed for the R148K mutant receptor, which reduced cAMP levels lower than that of pertussis toxin-treated samples, suggesting that the receptor inhibits the basal activity of adenylyl cyclase II (Fig. 1A). In Ltk− cells transfected with the R148K mutant, DPAT treatment did not alter basal or D1-induced cAMP, indicating deficient coupling to $G\alpha_i$ and lack of effect on G_s stimulation. Hence, the R148K mutant may prevent mobilization of $G\beta\gamma$, perhaps by binding free $G\beta\gamma$ subunits. Other mutants seemed to convert DPAT agonism to inverse or biased agonism, as suggested by DPAT-induced potentiation of dopamine-D1 receptor stimulation (Fig. 1B). For these mutants and wild-type 5-HT1A receptors, DPAT had no detectable effect on basal cAMP levels. Thus, coactivation of G_s by D1 receptor activation was required to observe DPAT-induced potentiation. This enhancement of D1 response was blocked by pertussis toxin treatment, indicating that the potentiation is mediated by G_i/G_o proteins and is not due to weak agonist-mediated stimulation of G_s, as observed for mutants of the 5-HT1A Ci3 domain (Malmberg and Strange, 2000). DPAT-induced potentiation was greatest for the P150T-5-HT1A receptor, which lacked coupling to adenylyl cyclase II. On the other hand, the R148K mutant that inhibited adenylyl cyclase II had no effect on D1-stimulated cAMP. Thus, distinct mutations of the Ci2 domain of the 5-HT1A receptor reduced basal activity or altered agonist function.

Functional 5-HT1A Mutants. Mutations at the Thr149 and Tyr144 sites, the most conserved residues in the Ci2 domain (Albert et al., 1998), resulted in receptors that retained the most complete coupling. The Thr149 mutants all coupled to $G\alpha_i$, and several retained $G\beta\gamma$ coupling, indicating that the polar hydroxyl residue of Thr149 is dispensable for

TABLE 2

Signaling phenotypes of mutant 5-HT1A receptors

Mutant 5-HT1A receptors were grouped according to their responses in the $G\alpha_i$-mediated (percentage of inhibition of dopamine-stimulated cAMP accumulation) and $G\beta\gamma$-mediated (DPAT-induced increase in intracellular calcium and $G\beta\gamma$-mediated stimulation of adenylyl cyclase II) assays. For $G\beta\gamma$ assays, the maximal response produced by wild-type 5-HT1A receptor was designated as 100%. Wild-type-like receptors include mutants with adenylyl cyclase II coupling of ≥50% and calcium mobilization ≥60% of wild-type 5-HT1A receptor, and inhibition of cAMP accumulation ≥30%. $G\alpha_i$-coupled/weak $G\beta\gamma$-coupled mutants include receptors that behave like the 5-HT1A-T149A receptor. These mutants had adenylyl cyclase II coupling of ≤30% and calcium mobilization that was 19 to 27% of that of wild-type 5-HT1A receptor and inhibition of cAMP accumulation of 24 to 53%. Uncoupled mutants had undetectable responses. $G\beta\gamma$-uncoupled mutants include receptors that were uncoupled from both $G\beta\gamma$ responses (calcium mobilization and adenylyl cyclase II) but still retained $G\alpha_i$ function (inhibition of cAMP). $G\beta\gamma$-selective coupled mutants include receptors that possess at least one intact $G\beta\gamma$ response. Receptors have been separated into two categories: 1) mutants that couple to adenylyl cyclase II stimulation; and 2) mutants that couple to phospholipase Cβ-mediated calcium mobilization. Several receptor mutants also displayed inverse activity. Some mutants inhibited the basal activity of adenylyl cyclase II, and others potentiated DPAT-induced D1 receptor stimulation to increase cAMP accumulation.

Ci2 Residue	Wild-Type-Like	$G\alpha_i$-Coupled/ Weak $G\beta\gamma$-Coupled	Uncoupled	$G\beta\gamma$-Uncoupled	$G\beta\gamma$-Selective Coupled		Inverse Basal Activity	
					ACII	PLCβ	ACII	Potentiation of DA-Stimulated [cAMP]
D143				D143C		D143F D143V D143N D143L		
Y144			Y144V Y144C	Y144H Y144I	Y144A Y144F	Y144N		Y144C
V145		V145L V145K	V145R V145S	V145Q V145E V145W				V145Y
N146	N146T			N146A		N146F		
K147			K147R K147Q					
R148		R148G	R148K R148V		R148P	R148L R148Q R148E	R148K	
T149	T149G T149R	T149A T149E T149Q		T149V T149M T149W	T149P			
P150			P150R P150N P150D P150G P150I P150L P150F P150S P150T				P150D	P150T P150N P150L P150G
R151		R151A R151T		R151Q R151M R151L R151K				
R152				R152V R152A		R152N R152P R152D		

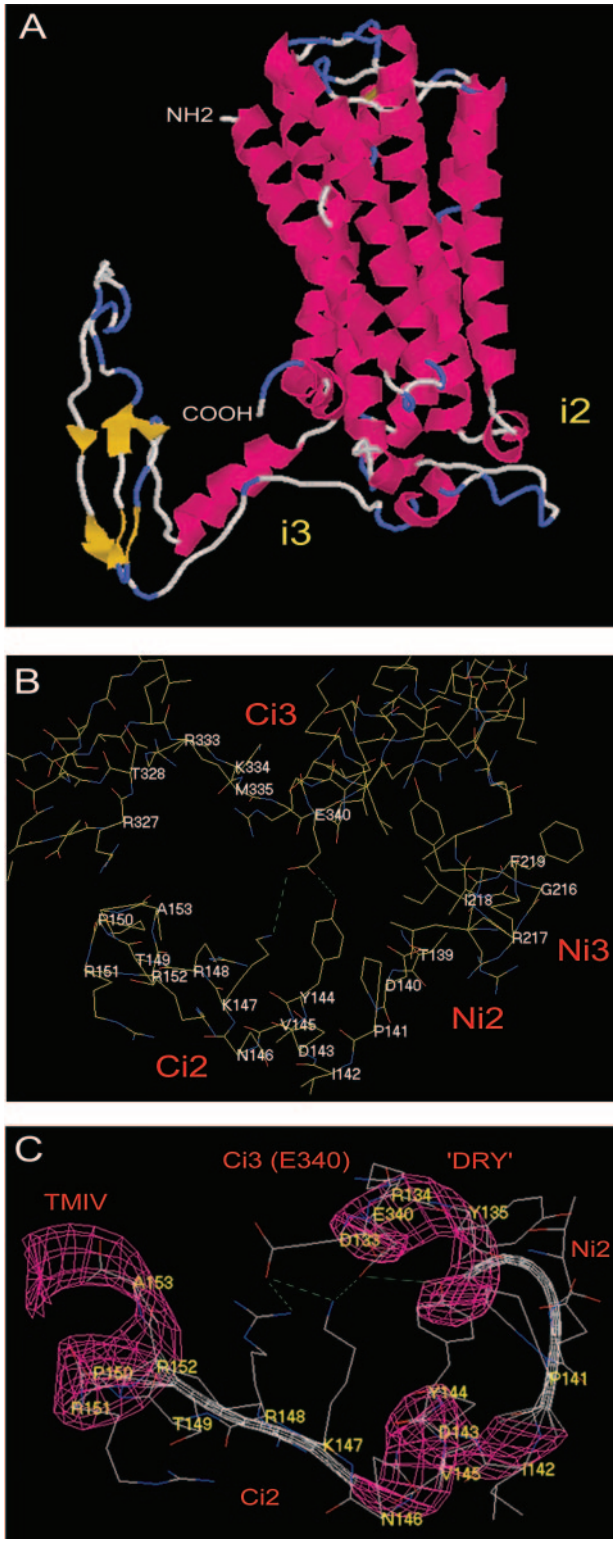

Fig. 3. Predicted structural model of the wild-type rat 5-HT1A receptor. The depicted model of the rat 5-HT1A receptor was based on the high-resolution crystal structure of bovine rhodopsin in its inactive state and homology with previously published 5-HT receptor models (Shapiro et al., 2002; Setola et al., 2005; see *Materials and Methods*) and was obtained using Protein Explorer (PE, http://www.proteinexplorer. org) and molecular mechanics energy calculations. A, side view of the wild-type 5-HT1A receptor. The α-helices are shown in pink, β-sheets are labeled with orange arrows, and the i2 and i3 loops are indicated. B, amino acids of the N- and C-terminal regions of the i2 and i3 loops (Ni2, Ni3, Ci2, and Ci3) are indicated. Potential interhelical ionic and/or hydrogen bonding between side chains of Ci3 residue Glu340 (E340) and Ci2 residues Tyr144/Lys147 (Y144/K147) are indicated by a broken green line. C, detailed view of the i2 loop domain showing secondary structure, α-helices are colored pink, and β-sheets are gray. Predicted coordinate hydrogen and ionic bonding of Tyr144/Lys147 (Ci2), Asp133/Arg134 (Ni2 DRY motif), and Glu340 (Ci3) is indicated as a green broken line.

coupling (Table 1 and Fig. 2). The T149G mutant coupled better to phospholipase C, whereas T149R coupled better to adenylyl cyclase II, indicating that G$\beta\gamma$ effector selectivity was affected by mutations at this site. The negatively charged T149E mutant, which mimics phosphothreonine, displayed weak G$\beta\gamma$ coupling but normal Gα_i coupling. Likewise, activation of protein kinase C, which phosphorylates the 5-HT1A receptor (Raymond, 1991) at several sites, including Thr149 (N. Kushwaha and P. R. Albert, unpublished data), selectively uncouples G$\beta\gamma$ signaling with little effect on Gα_i signaling (Lembo and Albert, 1995; Wu et al., 2002; Kushwaha and Albert, 2005). The results from Thr149 mutants displayed selective impairments of G$\beta\gamma$ signaling, indicating that the Thr149 site is critical for selective coupling of G$\beta\gamma$ subunits. Mutational analysis of the Tyr144 residue revealed that this is the most important Ci2 site in directing the coupling of 5-HT1A receptors to both Gα_i and G$\beta\gamma$ signaling. For example, the conservative Y144F mutation retained coupling to G$\beta\gamma$/adenylyl cyclase II and Gα_i but not to G$\beta\gamma$/phospholipase C, indicating a key role for the polar hydroxyl moiety of Tyr144 in coupling. The Y144A mutant coupled effectively to G$\beta\gamma$/adenylyl cyclase II but not to Gα_i or G$\beta\gamma$/phospholipase C, whereas the Y144N mutant coupled to Gα_i and G$\beta\gamma$/phospholipase C but not to G$\beta\gamma$/adenylyl cyclase II. This diversity of Tyr144 mutant signaling phenotypes indicates a critical role for the Tyr144 residue as a signaling terminus that is critical for the specificity of receptor coupling to Gα_i and G$\beta\gamma$.

Discussion

Structure-function studies of GPCR coupling to G-proteins have implicated the receptor i2 and i3 loops in G-protein activation, particularly the highly conserved N-terminal E/DRY i2 motif (Wess et al., 1997; Shapiro et al., 2002), but the role of the Ci2 domain is undetermined. Previous studies have examined primarily Gα-mediated signaling, but the structural determinants of G$\beta\gamma$-mediated signaling remain to be addressed (Bourne, 1997). Given that specific receptor- and effector-dependent G$\beta\gamma$ combinations mediate G$\beta\gamma$ signaling, accumulating data suggest that direct receptor-G$\beta\gamma$ interactions may underlie this specificity (Clapham and Neer, 1997; Chidiac, 1998; Albert and Robillard, 2002). We have examined the coupling of point mutants at each residue of the 5-HT1A Ci2 domain to Gα_i- or G$\beta\gamma$-mediated pathways. The majority of 5-HT1A-Ci2 mutant receptors displayed ligand binding that was comparable with that of wild-type receptors. However, most point mutants were uncoupled, either selectively from G$\beta\gamma$ or from both G$\beta\gamma$ and Gα_i signaling. This represents the first detailed evidence that the entire Ci2 domain plays a key role in receptor signaling to both G$\beta\gamma$ and Gα, which was unexpected, given the limited primary sequence homology of this domain (Albert et al., 1998). The sequence divergence of Ci2 domains may determine receptor-dependent G$\beta\gamma$ specificity.

Although mutations in the Ci2 domain did not affect the

predicted amphipathic α-helical secondary structure, mutations that altered the predicted coil localized at Pro150 resulted in completely uncoupled or inversely coupled receptors (Supplemental Table S2). The ACII assay provides a sensitive measure of ligand-independent 5-HT1A receptor activity that is sensitive to pertussis toxin and G$\beta\gamma$ scavengers, allowing for the determination constitutive activity (Albert et al., 1999). Two mutants displayed inverse basal activity toward ACII (R148K and P150D), whereas other mutants switched coupling of the full agonist DPAT to inverse agonism (Fig. 1B). It is noteworthy that substitutions at Pro150 generated receptors with inverse agonist properties at Gα_i or inverse basal coupling to G$\beta\gamma$ responses. The loss of the coil induced by mutations at Pro150 may transmit a general perturbation to completely inhibit weak basal activity the receptor.

To visualize the potential roles of the Ci2 domain residues in tertiary receptor structure, a computer model of the 5-HT1A receptor based on the X-ray crystal structure of bovine rhodopsin (Palczewski et al., 2000) was generated (Fig. 3). This model predicts that the Ci2 domain lies in close proximity to the Ni2, Ni3, and Ci3 portions of intracellular loops. In particular, the model predicts that Ci2 residues Tyr144 and Lys147 lie in close proximity to Ci3 residue Glu340, possibly forming hydrogen, van der Waals, or ionic bonds. Viewed from a rotated angle (Fig. 3C), it becomes apparent that Lys147 and Arg148 are in close proximity to Asp133 and could interact with the conserved DRY motif—perhaps via ionic or other types of interactions. The Arg134 site is also predicted to be near enough to Glu340 (Ci3) to facilitate intramolecular interactions between Ni2 (DRY motif), Ci2 (YXXKR motif), and Ci3 (Glu340). A similar network of interactions between i2 and Ci3 via the DRY motif and the homologous Glu318 residue of the 5-HT2A receptor has been noted previously (Shapiro et al., 2002). The lack of coupling of the K147R- and R148R- 5-HT1A receptors suggests that the ϵ-amino or guanidinium side chains of these residues make specific, spatially restricted interactions. Mutations of Tyr144 showed the greatest diversity of coupling phenotypes (depending on the substitution), suggesting that this site not only stabilizes receptor coupling domains but may have direct interactions with G$\beta\gamma$ subunits to determine signaling selectivity. The YXXKR motif is absolutely conserved in all 5-HT1A receptor homologs (to *Caenorhabditis elegans*) and in several 5-HT1, muscarinic (M1–M5), and adrenergic (α2) receptors, and the Tyr144 residue is highly conserved among class I GPCRs (Albert et al., 1998), suggesting a conserved role in these receptors. Our data support the importance of the YXXKR residues in determining the efficiency and selectivity 5-HT1A receptor coupling.

Our previous studies had implicated Thr149 in G$\beta\gamma$ coupling of the 5-HT1A receptor (Lembo et al., 1997; Albert et al., 1999; Wu et al., 2002; Kushwaha and Albert, 2005) and Thr149 mutants all retained coupling to Gα_i but were selectively uncoupled from G$\beta\gamma$. For example, the T149G mutant coupled better to phospholipase Cβ-mediated calcium mobilization than to stimulation of ACII, whereas the T149R mutant coupled better to ACII than to phospholipase Cβ. The polar hydroxyl group of Thr149 seems to project outward from hydrophilic face of the receptor (Fig. 3C) and may stabilize G$\beta\gamma$ binding to the receptor. Likewise, Asn146 and Asp143 mutations also retained coupling to Gα_i but had selective impairments in G$\beta\gamma$ signaling. Like Thr149, the side chains of these residues are polar and are also predicted to project outward to the cytoplasm (Fig. 3, B and C) and may stabilize G$\beta\gamma$ interactions. In summary, our data are consistent with a model of positively charged residues in the 5-HT1A-Ci2 domain that create a hydrophilic face which permits specific interactions of polar side chains of Asp143, Asn146, and Thr149 to mediate G$\beta\gamma$ coupling.

In contrast to the 5-HT1A Ci2 domain, the i3 loop (Ni3 and Ci3) has been implicated in G-protein signaling but mainly in coupling to Gα_i. Peptides corresponding to the 5-HT1A Ci3 domain mimic Gα_i-mediated inhibition of forskolin-stimulated AC and attenuate inhibitory coupling of 5-HT1A receptors to AC (Malmberg and Strange, 2000; Ortiz et al., 2000). Likewise, 5-HT1A-i2 loop peptides mediate direct coupling to inhibition of cAMP (Varrault et al., 1994). Mutation of Ci3 residues (V344E and T343A/V344E) enhanced receptor coupling to G_s over G_i, consistent with its role in determining Gα_i specificity (Malmberg and Strange, 2000). Thus, whereas Ci3 seems to mainly dictate Gα_i specificity, our results indicate that Ci2 is mainly implicated in G$\beta\gamma$ signaling but also contributes to Gα_i signaling. The C-terminal domain of the 5-HT1A receptor also seems to be critical for coupling to both Gα_i and G$\beta\gamma$ pathways. Unlike other receptors, the 5-HT1A receptor is constitutively palmitoylated at C-terminal cysteine residues (417 and 420), and palmitoylation is required for coupling to G_i (i.e., loss of inhibition of AC activity) and G$\beta\gamma$-mediated activation of extracellular signal-regulated kinases (Papoucheva et al., 2004). Thus, Ci2, Ni3, Ci3, and palmitoylated 5-HT1A C-terminal domains seem critical for G-protein coupling and may directly interact to form a G-protein coupling interface.

In summary, our mutagenesis studies show that multiple residues in the Ci2 sequence ^{143}DYVNKRTPRR^{152} are implicated in 5-HT1A receptor coupling to G$\beta\gamma$ and Gα_i. The pattern of mutations indicates that the positively charged face of the predicted amphipathic Ci2 α-helix is absolutely required for coupling and that uncharged residues in this face (Thr149, Asn146) direct G$\beta\gamma$ but not Gα_i coupling. The opposite inwardly oriented face includes a critical Tyr144 residue that directs the specificity of coupling to both G$\beta\gamma$ and Gα_i pathways and interacts with the Ci3 or Ni2 loops, forming the G-protein coupling interface.

Acknowledgments

We thank Dr. Bryan Roth for generating the atomic coordinate file for the rat 5-HT1A receptor.

References

Albert PR and Lemonde S (2004) 5-HT1A receptors, gene repression and depression: guilt by association. *Neuroscientist* **10:**575–593.

Albert PR, Morris SJ, Ghahremani MH, Storring JM, and Lembo PM (1998) A putative alpha-helical G beta gamma-coupling domain in the second intracellular loop of the 5-HT1A receptor. *Ann NY Acad Sci* **861:**146–161.

Albert PR and Robillard L (2002) G protein specificity. Traffic direction required. *Cell Signal* **14:**407–418.

Albert PR, Sajedi N, Lemonde S, and Ghahremani MH (1999) Constitutive G_{i2}-dependent activation of adenylyl cyclase type II by the 5-HT1A receptor. Inhibition by anxiolytic partial agonists. *J Biol Chem* **274:**35469–35474.

Ballesteros JA, Jensen AD, Liapakis G, Rasmussen SG, Shi L, Gether U, and Javitch JA (2001) Activation of the β2-adrenergic receptor involves disruption of an ionic lock between the cytoplasmic ends of transmembrane segments 3 and 6. *J Biol Chem* **276:**29171–29177.

Bourne HR (1997) How receptors talk to trimeric G proteins. *Curr Opin Cell Biol* **9:**134–142.

Burstein ES, Spalding TA, and Brann MR (1996) Amino acid side chains that define muscarinic receptor/G-protein coupling. Studies of the third intracellular loop. *J Biol Chem* **271:**2882–2885.

Burstein ES, Spalding TA, and Brann MR (1998) The second intracellular loop of the m5 muscarinic receptor is the switch which enables G-protein coupling. *J Biol Chem* **273:**24322–24327.

Chidiac P (1998) Rethinking receptor-G protein-effector interactions. *Biochem Pharmacol* **55:**549–556.

Clapham DE and Neer EJ (1997) G protein beta gamma subunits. *Ann Rev Pharmacol Toxicol* **37:**167–203.

Gross C and Hen R (2004) The developmental origins of anxiety. *Nat Rev Neurosci* **5:**545–552.

Hill-Eubanks D, Burstein ES, Spalding TA, Brauner-Osborne H, and Brann MR (1996) Structure of a G-protein-coupling domain of a muscarinic receptor predicted by random saturation mutagenesis. *J Biol Chem* **271:**3058–3065.

Kushwaha N and Albert PR (2005) Coupling of 5-HT1A autoreceptors to inhibition of mitogen-activated protein kinase activation via Gbetagamma subunit signaling. *Eur J Neurosci* **21:**721–732.

Lembo PM and Albert PR (1995) Multiple phosphorylation sites are required for pathway-selective uncoupling of the 5-hydroxytryptamine1A receptor by protein kinase C. *Mol Pharmacol* **48:**1024–1029.

Lembo PM, Ghahremani MH, Morris SJ, and Albert PR (1997) A conserved threonine residue in the second intracellular loop of the 5- hydroxytryptamine 1A receptor directs signaling specificity. *Mol Pharmacol* **52:**164–171.

Liu J, Conklin BR, Blin N, Yun J, and Wess J (1995) Identification of a receptor/G-protein contact site critical for signaling specificity and G-protein activation. *Proc Natl Acad Sci USA* **92:**11642–11646.

Liu YF and Albert PR (1991) Cell-specific signaling of the 5-HT1A receptor. Modulation by protein kinases C and A. *J Biol Chem* **266:**23689–23697.

Liu YF, Ghahremani MH, Rasenick MM, Jakobs KH, and Albert PR (1999) Stimulation of cAMP Synthesis by G_i-coupled receptors upon ablation of distinct $G\alpha_i$ protein expression. Gi subtype specificity of the 5-HT1A receptor. *J Biol Chem* **274:**16444–16450.

Malmberg A and Strange PG (2000) Site-directed mutations in the third intracellular loop of the serotonin 5-HT_{1A} receptor alter G protein coupling from G_i to G_s in a ligand-dependent manner. *J Neurochem* **75:**1283–1293.

Meng EC and Bourne HR (2001) Receptor activation: what does the rhodopsin structure tell us? *Trends Pharmacol Sci* **22:**587–593.

Ortiz TC, Devereaux MC Jr, and Parker KK (2000) Structural variants of a human 5-HT1a receptor intracellular loop 3 peptide. *Pharmacology* **60:**195–202.

Palczewski K, Kumasaka T, Hori T, Behnke CA, Motoshima H, Fox BA, Le Trong I, Teller DC, Okada T, Stenkamp RE, et al. (2000) Crystal structure of rhodopsin: a G protein-coupled receptor. *Science (Wash DC)* **289:**739–745.

Papoucheva E, Dumuis A, Sebben M, Richter DW, and Ponimaskin EG (2004) The 5-hydroxytryptamine$_{1A}$ receptor is stably palmitoylated and acylation is critical for communication of receptor with Gi protein. *J Biol Chem* **279:**3280–3291.

Pineyro G and Blier P (1999) Autoregulation of serotonin neurons: role in antidepressant drug action. *Pharmacol Rev* **51:**533–591.

Raymond JR (1991) Protein kinase C induces phosphorylation and desensitization of the human 5-HT1A receptor. *J Biol Chem* **266:**14747–14753.

Sakmar TP, Menon ST, Marin EP, and Awad ES (2002) Rhodopsin: insights from recent structural studies. *Annu Rev Biophys Biomol Struct* **31:**443–484.

Schmidt C, Li B, Bloodworth L, Erlenbach I, Zeng FY, and Wess J (2003) Random mutagenesis of the M3 muscarinic acetylcholine receptor expressed in yeast. Identification of point mutations that "silence" a constitutively active mutant M3 receptor and greatly impair receptor/G protein coupling. *J Biol Chem* **278:**30248–30260.

Setola V, Dukat M, Glennon RA, and Roth BL (2005) Molecular determinants for the interaction of the valvulopathic anorexigen norfenfluramine with the 5-HT2B receptor. *Mol Pharmacol* **68:**20–33.

Shapiro DA, Kristiansen K, Weiner DM, Kroeze WK, and Roth BL (2002) Evidence for a model of agonist-induced activation of 5-hydroxytryptamine 2A serotonin receptors that involves the disruption of a strong ionic interaction between helices 3 and 6. *J Biol Chem* **277:**11441–11449.

Shi L, Liapakis G, Xu R, Guarnieri F, Ballesteros JA, and Javitch JA (2002) β2 Adrenergic receptor activation. Modulation of the proline kink in transmembrane 6 by a rotamer toggle switch. *J Biol Chem* **277:**40989–40996.

Spalding TA, Burstein ES, Henderson SC, Ducote KR, and Brann MR (1998) Identification of a ligand-dependent switch within a muscarinic receptor. *J Biol Chem* **273:**21563–32568.

Sun QQ and Dale N (1999) G-proteins are involved in 5-HT receptor-mediated modulation of N- and P/Q- but not T-type Ca^{2+} channels. *J Neurosci* **19:**890–899.

Thiagaraj HV, Ortiz TC, Burnett A, and Parker KK (2002) G protein coupling and activation characteristics of intracellular loops 2 and 3 of the 5-HT1a receptor. *Trends Compar Biochem Physiol* **9:**117–129.

Turner JH, Gelasco AK, and Raymond JR (2004) Calmodulin interacts with the third intracellular loop of the serotonin 5-hydroxytryptamine1A receptor at two distinct sites: putative role in receptor phosphorylation by protein kinase C. *J Biol Chem* **279:**17027–17037.

Varrault A, Le Nguyen D, McClue S, Harris B, Jouin P, and Bockaert J (1994) 5-Hydroxytryptamine1A receptor synthetic peptides. Mechanisms of adenylyl cyclase inhibition. *J Biol Chem* **269:**16720–16725.

Wess J, Liu J, Blin N, Yun J, Lerche C, and Kostenis E (1997) Structural basis of receptor/G protein coupling selectivity studied with muscarinic receptors as model systems. *Life Sci* **60:**1007–1014.

Wu X, Kushwaha N, Albert PR, and Penington NJ (2002) A critical protein kinase C phosphorylation site on the 5-HT_{1A} receptor controlling coupling to N-type calcium channels. *J Physiol* **538:**41–51.

Wurch T, Colpaert FC, and Pauwels PJ (2003) Mutation in a protein kinase C phosphorylation site of the 5-HT_{1A} receptor preferentially attenuates Ca^{2+} responses to partial as opposed to higher-efficacy 5-HT_{1A} agonists. *Neuropharmacology* **44:**873–881.

Zeng FY, Hopp A, Soldner A, and Wess J (1999) Use of a disulfide cross-linking strategy to study muscarinic receptor structure and mechanisms of activation. *J Biol Chem* **274:**16629–16640.

Address correspondence to: Dr. Paul R. Albert, Ottawa Health Research Institute (Neurosciences), 451 Smyth Road, Ottawa, Ontario, Canada, K1H 8M5. E-mail: palbert@uottawa.ca